ECERTA

Enabling Certification by Analysis

___

Marie Curie Excellence Team

Start: 01 January 2007
Duration: 48 months

www.cfd4aircraft.com

Modelling of structural damping

Prepared by: **Marco Prandina**

Document control data

Deliverable No.:	D **5.1**	Due date:	**01 October 2007**
Version:	**Draft Version 2**	Team Leader:	**Prof. Ken Badcock**
Date delivered:	**25 October 2007**	Host Organisation : University of Liverpool	

1 Introduction

Damping is the dissipation of energy from a vibrating structure [1] or the energy dissipating property of materials and members undergoing time dependant deformations and/or displacements [2].

Damping can be classified into three main categories [3]:

Material damping: the energy dissipation due to microstructural mechanisms as irreversible intercrystal heat flux, grain boundary viscosity, etc.
Boundary damping: the dissipation associated with junctions or interfaces between parts of the structure (joints) and contacting surfaces (friction).
Fluid contact damping: the energy radiation into surrounding medium and dissipation associated with local viscous effects.

Damping is often neglected or over-simplified in dynamic design and modelling of structures. However, there are many cases where an accurate identification of structural damping is very important, especially when the dynamics is dominated by the energy dissipation.
If a model is to be used to predict transient responses, transmissibility of exciting forces through the structure or decay times, good modelling of damping is necessary. The flutter problem in aircraft wings is an example of a phenomenon dominated by energy dissipation, where damping prediction is important.
Unfortunately, damping is still one of the least well-understood aspects of vibration analysis for many reasons. First, there is an absence of a universal mathematical model to represent all damping forces. Secondly, it is not clear which state variables the damping forces will depend on. Mechanisms that dissipate energy in a system are very different both in nature and effect, and engineering choices must be made before starting to develop a model. Finally, damping parameters cannot be measured by the static tests used for stiffness and inertia; dynamic tests, which are normally more effected by noise, are needed.
An important consideration in the current work, which is aimed at the prediction of the aeroelastic response of aircraft, is the ability to model damping in large structures. Computational efficiency is important and it may be difficult to include all sources of damping in detail.
This report describes results obtained by initial experiments with several models derived from the literature and proposes a new method based on orthogonality equations of the symmetric definite quadratic pencil.
Firstly, the importance of damping in aeroelasticity is discussed. Secondly a background review on some mathematical models is presented in order to introduce two identification methods that have been described and numerically tested.
Then, the new method based on orthogonality equations of the symmetric definite quadratic pencil is proposed and tested on the same numerical example. The proposed method is then compared with the two other methods by introducing two measures of error.
Finally, the principle conclusions of this research and suggestions for future work are presented.

2 Damping in aeroelasticity

The problem of modelling damping in structures is not well-understood because often in traditional structural design it is not actually important, mainly because there are no instabilities and there is no reason to accurately model it. In the aeroelastic problem, instead, the occurrence of instabilities may strongly depend on damping and catastrophic events can occur.

Flutter is a characteristic form of self-excited oscillations that can arise through the interaction of an aerodynamic flow with the elastic modes of a mechanical structure, e.g. the bending and torsion modes of an aircraft wing.

The occurrence of flutter compromises the operational safety, flight performance and energy efficiency of the aircraft. By definition, flutter phenomenon can be defined as the dynamic instability of a structure in an air stream, characterized by the interactions of elastic deformation and aerodynamic loads [4].

Consider a cantilever wing mounted in a wind tunnel and with the root rigidly attached to the tunnel wall. Suppose that the wing is deliberately deflected and then released. When the wind speed is low, the oscillatory motion of the wing is damped; as the wind speed is increased up to a certain level, the rate of damping will increase but thereafter will decrease as the speed increases. Eventually, if the available wind speed is high enough, the oscillation will cease to be damped and a limit cycle oscillation can be maintained. This is the critical condition and the wind speed is the critical flutter speed for that wing. In general, at a wind speed a little above the critical condition the oscillation will be divergent, i.e. its amplitude will increase with time [5].

From the structural point of view, the main sources of damping in a wing are the friction in joints, viscous damping due to air flow and material damping.

Modelling of damping is a very difficult issue because the level of damping in a structure can depend, for example, on the material damping that is dependent on the type of the material, the methods used in manufacturing the material and the final finishing processes. The interfacial damping mechanism, instead, results from Coulomb friction between members and connections and can depend on clamp force of bolts or welded connections.

For all these reasons, normally the identification is preferred to modelling because trying to extract damping parameters by experiments is simpler than collecting all the information to model damping accurately.

It's important to start from the fundamentals of identification in order to obtain a method that is applicable to Ground Vibration Test normally used in aeroelasticity.

3 Background review

One of the first attempts to model damping was made by Rayleigh in his monograph "Theory of sound" [6] in 1877. The so-called "viscous damping" supposes that instantaneous generalized velocities are the only relevant state variables which influence damping.

For a single degree of freedom system, the equation of motion becomes

$$m\ddot{x} + c\dot{x} + k\,x = f(t) \tag{1}$$

where m and k are respectively the mass and stiffness coefficients, responsible for inertia and elastic forces, $f(t)$ and x the excitation force applied to the system and the corresponding displacement response; c is the damping coefficient that encapsulates all damping sources and is responsible for dissipative forces.

This model is probably the simplest to represent damping forces, and for some systems is a good approximation, especially when fluid viscosity is the main energy dissipation mechanism.

Expanding the problem to an n-degree of freedom system, the equations of motion can be written in a matrix form as

$$\mathbf{M}\,\ddot{\mathbf{q}} + \mathbf{C}\,\dot{\mathbf{q}} + \mathbf{K}\,\mathbf{q} = \mathbf{f}(t) \tag{2}$$

where $\mathbf{M}$ and $\mathbf{K}$ are respectively mass and stiffness which are n x n definite positive matrices, responsible for inertia and elastic forces, $\mathbf{f}(t)$ and $\mathbf{q}$ the vector of the excitation forces applied to each degree of freedom and the corresponding vector of displacement responses; $\mathbf{C}$ is the n x n semi-definite positive viscous damping matrix.

With the separation of variables

$$\mathbf{q}(t) = \mathbf{x}\,e^{\lambda t} \tag{3}$$

the solutions of eq.(2) can be found by solving the eigenproblem related to the second order quadratic pencil

$$P(\lambda) = \lambda^2 \mathbf{M} + \lambda \mathbf{C} + \mathbf{K} \tag{4}$$

The eigenvalues and the eigenvectors of the second order pencil are respectively the non-zero scalar λ_i and the corresponding vector $\mathbf{x}_i$ that satisfies

$$P(\lambda_i)\,\mathbf{x}_i = \left(\lambda_i{}^2 \mathbf{M} + \lambda_i \mathbf{C} + \mathbf{K}\right)\mathbf{x}_i = 0 \tag{5}$$

In order to obtain real eigenvalues and eigenvectors from eq.(5), so the equations of motion can be decoupled as for the undamped case, Rayleigh proposed the "proportional damping" model.

Proportional damping may be defined as a dissipative situation where the viscous damping matrix $\mathbf{C}$ is directly proportional to either the stiffness or mass matrix, or to a linear combination of both [7].

Considering the more general case of proportional damping, we may write

$$\mathbf{C} = \varepsilon\,\mathbf{K} + \nu\,\mathbf{M} \tag{6}$$

where ε and ν are constants.

Using this model it is now possible to derive n uncoupled damped single degree of freedom equations each of which can be solved separately from the others.

However, there is no physical reason why the damping matrix has to be proportional to the mass and stiffness matrices. Also, eigenvalues and eigenvectors of damped systems measured from real experiments always lead to complex quantities, so this model is just a mathematical way to apply the classic modal undamped analysis to the damped one.

This fact gives the idea that damping can be extracted in some way from the imaginary part of eigenvectors (or complex mode shapes) and eigenvalues (or complex frequencies).

4   Identifying the damping matrix

4.1   Adhikari's method

In reference [8] a method is presented which is based on the first order perturbational method. This method assumes that the damping is small, so eigenvalues and eigenvectors of the damped system will be close to the undamped ones.
The data needed to identify the damping viscous matrix are just the complex frequencies (eigenvalues) and mode shapes (eigenvectors) measured by normal modal experiments. Defining:

$\mathbf{x}_i$ =   mode shapes of the undamped system (real)
$\mathbf{z}_i$ =   mode shapes of the damped system (complex)
ω_i =   natural frequencies of the undamped system (real)
λ_i =   complex frequencies of the damped system (complex)

under the assumption of "small damping", the following approximation can be used:

$$\mathbf{z}_j = \sum_{l=1}^{N} \alpha_l^{(j)} \mathbf{x}_l \quad \text{where} \quad \alpha_j^{(j)} = 1 \quad \text{and} \quad \left|\alpha_l^{(j)}\right| << 1 \quad \forall\, l \neq j \qquad (7)$$

By saying $\alpha_j^{(j)} = 1$ and all other coefficients $\alpha_l^{(j)} << 1$ is meant that the jth damped mode $\mathbf{z}_j$ is close to the corresponding undamped mode $\mathbf{x}_j$ and the contribution given by all other modes is small.
With the separation of variables

$$\mathbf{q}(t) = \mathbf{z}\, e^{i\lambda t} \qquad (8)$$

applied to eq.(2), a new quadratic pencil is obtained in the form

$$-\lambda_j^{2} \mathbf{M}\, \mathbf{z}_j + i\lambda_j \mathbf{C}\, \mathbf{z}_j + \mathbf{K}\, \mathbf{z}_j = 0 \qquad (9)$$

Substituting $\mathbf{z}_j$ from eq.(7) and premultiplying by $\mathbf{x}_k^{\mathrm{T}}$ and using the orthogonality properties of the undamped mode shapes we obtain

$$-\lambda_j^{2} \alpha_k^{(j)} + i\lambda_j \sum_{l=1}^{N} \alpha_l^{(j)} C'_{kl} + \omega_k^{2} \alpha_k^{(j)} = 0 \qquad (10)$$

where

$$C'_{kl} = \mathbf{x}_k^{T} \mathbf{C}\, \mathbf{x}_l \qquad (11)$$

Now, for the case $k = l$, neglecting the second order terms involving $\alpha_l^{(j)}$ and C'_{kl}, $\forall\ k \neq l$, we obtain

$$\lambda_j \approx \pm\omega_j + \frac{iC'_{jj}}{2} \tag{12}$$

and for the case $k \neq l$, again retaining only the first order terms, we obtain

$$\mathbf{z}_j \approx \mathbf{x}_j + i\sum_{\substack{k=1\\k\neq j}}^{N} \frac{\omega_j C'_{kj}}{\omega_j^2 - \omega_k^2} \mathbf{x}_k \tag{13}$$

From the imaginary part of experimental complex eigenvalues and eigenvectors, using eqs.(12) and (13), it is now possible to extract the $\mathbf{C'}$ matrix in modal coordinates and then convert it to the original coordinate system by the relation

$$\mathbf{C} = \left(\mathbf{X}^T\right)^{-1}\mathbf{C'}\mathbf{X}^{-1} \tag{14}$$

The Adhikari's method does not guarantee symmetry in the fitted damping matrix and non-physical results may be obtained, because the original system is reciprocal. The same author proposed a different model [9] based on the same considerations of the original one (first order perturbational method) that preserves reciprocity of the system forcing

$$C'_{kj} = C'_{jk} \tag{15}$$

This method gives better results because is known that the original system is reciprocal and then it is possible to reduce the uncertainties about the damping matrix including this further constraint.
A very similar method was also proposed in reference [10] using the perturbation analysis for complex modes.

4.2   Pilkey's method

Another approach to identification of damping was proposed in reference [11]. The method is based on Lancaster's work on the quadratic pencil [12] and on the inversion of lambda-matrices and application to the theory of vibrations [13]. It presents two methods (one iterative and one direct) for the identification of the viscous damping matrix in a dynamical system.
Two assumptions are made in this paper: $\mathbf{M}$, $\mathbf{C}$ and $\mathbf{K}$ are symmetric ($\mathbf{M}$ is positive definite) and damping is subcritical, so eigenvalues and eigenvectors arise in complex conjugate pairs.
The data needed for this model to identify damping are the complex frequencies (eigenvalues) and mode shapes (eigenvectors) from experiments and the $\mathbf{M}$ matrix for the iterative method. For the direct method, also the $\mathbf{K}$ matrix must be known.
This method considers the second order pencil eigenvalues equation (5) rearranged in the Duncan state-space form

$$\left\{\lambda_i \begin{bmatrix} \mathbf{0} & \mathbf{M} \\ \mathbf{M} & \mathbf{C} \end{bmatrix} + \begin{bmatrix} -\mathbf{M} & \mathbf{0} \\ \mathbf{0} & \mathbf{K} \end{bmatrix}\right\} \begin{pmatrix} \lambda_i \mathbf{x}_i \\ \mathbf{x}_i \end{pmatrix} = \mathbf{0} \tag{16}$$

The eigenvectors can be normalized so that

$$\begin{bmatrix} \mathbf{\Lambda X}^T & \mathbf{X}^T \end{bmatrix} \begin{bmatrix} \mathbf{0} & \mathbf{M} \\ \mathbf{M} & \mathbf{C} \end{bmatrix} \begin{bmatrix} \mathbf{X\Lambda} \\ \mathbf{X} \end{bmatrix} = \mathbf{I} \tag{17}$$

where

$$\mathbf{\Lambda} = diag(\lambda_i) \in C^{2n \times 2n} \tag{18}$$

$$\mathbf{X} = \begin{bmatrix} x_1 \, x_2 \ldots x_{2n} \end{bmatrix} \in C^{n \times 2n} \tag{19}$$

Another orthogonality relation can be written as

$$\begin{bmatrix} \mathbf{\Lambda X}^T & \mathbf{X}^T \end{bmatrix} \begin{bmatrix} -\mathbf{M} & \mathbf{0} \\ \mathbf{0} & \mathbf{K} \end{bmatrix} \begin{bmatrix} \mathbf{X\Lambda} \\ \mathbf{X} \end{bmatrix} = -\mathbf{\Lambda} \tag{20}$$

From the eigenvector normalization equations (17) and (20) we can extract two normalization conditions for the iterative and the direct method respectively,

$$x_i^T (2\mathbf{M}\lambda_i + \mathbf{C}) x_i = 1 \tag{21}$$

$$x_i^T (\mathbf{M}\lambda_i^2 - \mathbf{K}) x_i = \lambda_i \tag{22}$$

Eq.(21) is used in the iterative method because the **C** matrix, which is the one that has to be identified, is not known when the normalization is performed for the first time. So after an initial guess, iteration is necessary in order to identify the **C** matrix until the error between successive damping matrices is small enough to imply convergence.
At the same time, eq.(22) is used in the direct method without iteration, but the **K** matrix must be known.
From equation (17) we get

$$\left(\begin{bmatrix} \mathbf{\Lambda X}^T & \mathbf{X}^T \end{bmatrix} \begin{bmatrix} \mathbf{0} & \mathbf{M} \\ \mathbf{M} & \mathbf{C} \end{bmatrix} \begin{bmatrix} \mathbf{X\Lambda} \\ \mathbf{X} \end{bmatrix} \right)^{-1} = \mathbf{I} \tag{23}$$

and expanding the inverse on the right hand side and rearranging leads to

$$\begin{bmatrix} \mathbf{0} & \mathbf{M} \\ \mathbf{M} & \mathbf{C} \end{bmatrix}^{-1} = \begin{bmatrix} \mathbf{X\Lambda} \\ \mathbf{X} \end{bmatrix} \begin{bmatrix} \mathbf{\Lambda X}^T & \mathbf{X}^T \end{bmatrix} \tag{24}$$

or

$$\begin{bmatrix} \mathbf{0} & \mathbf{M} \\ \mathbf{M} & \mathbf{C} \end{bmatrix}^{-1} = \begin{bmatrix} \mathbf{X}\mathbf{\Lambda}^2\mathbf{X}^T & \mathbf{X}\mathbf{\Lambda}\mathbf{X}^T \\ \mathbf{X}\mathbf{\Lambda}\mathbf{X}^T & 0 \end{bmatrix} \qquad (25)$$

It can be proven that the left hand side matrix inverse is

$$\begin{bmatrix} \mathbf{0} & \mathbf{M} \\ \mathbf{M} & \mathbf{C} \end{bmatrix}^{-1} = \begin{bmatrix} -\mathbf{M}^{-1}\mathbf{C}\mathbf{M}^{-1} & \mathbf{M}^{-1} \\ \mathbf{M}^{-1} & 0 \end{bmatrix} \qquad (26)$$

By comparing the right hand sides in eqs.(25) and (26)

$$-\mathbf{M}^{-1}\mathbf{C}\mathbf{M}^{-1} = \mathbf{X}\mathbf{\Lambda}^2\mathbf{X}^T \qquad (27)$$

which gives

$$\mathbf{C} = -\mathbf{M}\mathbf{X}\mathbf{\Lambda}^2\mathbf{X}^T\mathbf{M} \qquad (28)$$

5   Numerical problems

There are some practical issues in solving the inverse problem of damping identification for a real structure, the most important being:

- Spatial and modal incompleteness of data
- Ill-conditioning of matrices
- Non-uniqueness of solutions
- Computational time for large structural models
- Noise and errors in measurement

The spatial incompleteness of data occurs when the number of degrees of freedom (dof) measurable by experiments is less than the number of dof in the finite element model (FEM). Normally a FEM has thousands of dof but in experiments just a few accelerometers are usually available and rotational dof are very hard to measure. To avoid this type of incompleteness, several reduction techniques were developed to reduce system matrices to the number of measurable dof (Guyan or Static Reduction [15], Dynamic Reduction [16], Improved Reduced System IRS [17], System Equivalent Reduction Expansion Process SEREP [18]) or to expand the data obtained from experiments to the dof of the FEM (using mass and stiffness matrices or using modal data [14]).

Modal incompleteness, instead, deals with the frequency range of measurements. Normally only some mode shapes and natural frequencies can be accurately measured because of noise and other factors, especially at high frequencies. For this reason, the number of mode shapes available for identification is always smaller than the number of mode shapes available in theory.

Ill-conditioning of matrices is another important issue when dealing with real data. In inverse problems this arises when an inversion of the matrix has to be made and some columns or rows of the matrix are close to being linearly dependent or very different in

amplitude. This can result in errors in identification of damping parameters and well-conditioning optimization techniques can be necessary.

Non-uniqueness of solutions arises when the number of equations available is less than the number of unknowns and so it is possible to have different solutions that solve the problem. A solution to this phenomenon can be adding redundant equations derived from the original ones or introduce constraints based on engineering knowledge.

6   Numerical tests

In order to evaluate how much existing methods are affected by numerical problems, some numerical tests were performed using MATLAB codes. The first analyzed problem is the modal incompleteness of data that always occurs in experiments with real structures.
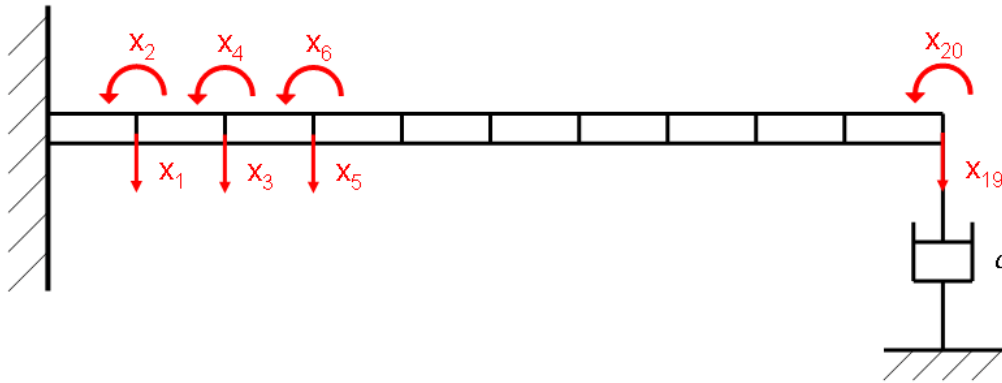

Figure 1 - **Ten-element FEM of a clamped beam with viscous dashpot on its free end**

The modal incompleteness of data has been included in numerical testing on a simple structure: a ten-element FEM of a clamped beam with a viscous dashpot on its free end (Figure 1).

A clamped ten-element beam with 22 dof (2 of them constraints by the clamp) has 20 analytical natural frequencies and 20 mode shapes.

The known mass, stiffness and damping matrices of the FEM were used to calculate eigenvalues and eigenvectors of the problem, using the Duncan state-space equations. Then, to simulate modal incompleteness of data from experiments, just some of the frequencies and mode shapes obtained were used for the identification inverse problem.

In this system, the viscous damping matrix has the form

$$\mathbf{C} = \begin{bmatrix} 0 & ... & ... & ... & ... & 0 \\ ... & ... & & & & ... \\ ... & & ... & & & ... \\ ... & & & ... & & ... \\ ... & & & & c & ... \\ 0 & ... & ... & ... & ... & 0 \end{bmatrix} \tag{29}$$

All components of **C** are zero except for the value of the damping coefficient of the viscous dashpot in the 19th row and column. This is illustrated in Figure 2.

The results were obtained using the symmetry variation of Adhikari's method and the Pilkey's direct method. The results obtained using respectively all 20 modes, the first 15 and the first 10 are shown in figures 3-5.

Using all the information available (Figure 3), both methods work perfectly as expected using numerical data. When the number of modes available decrease (Figure 4) Adhikari's method starts showing some problems: the biggest value of the damping matrix is not in the right place and there are many off-diagonal elements very far from the exact solution.
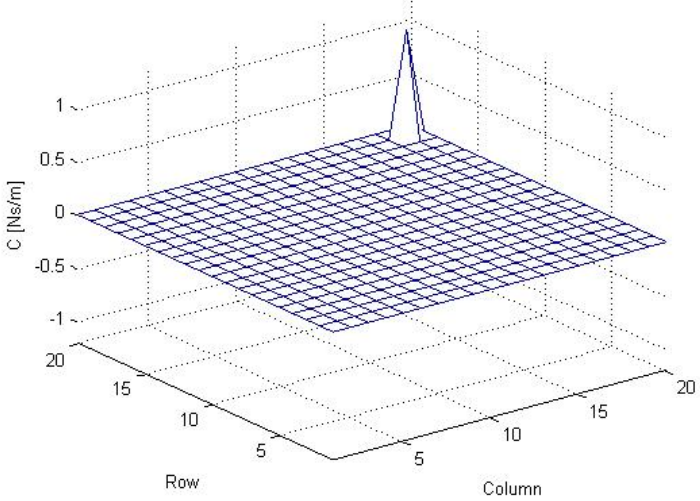

Figure 2 - Graphical representation of the viscous damping matrix

Surprisingly, further reduction in the number of modes available used in Adhikari's method seems to reduce the error (Figure 5), matching again the right column and row for the biggest value, but still showing many wrong values.
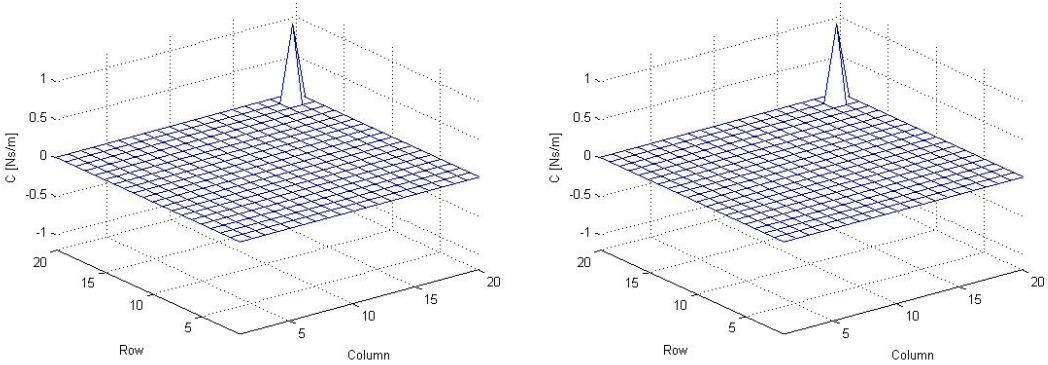

Figure 3 - Damping matrix by Adhikari's method (left) and Pilkey's method (right), 20/20 modes
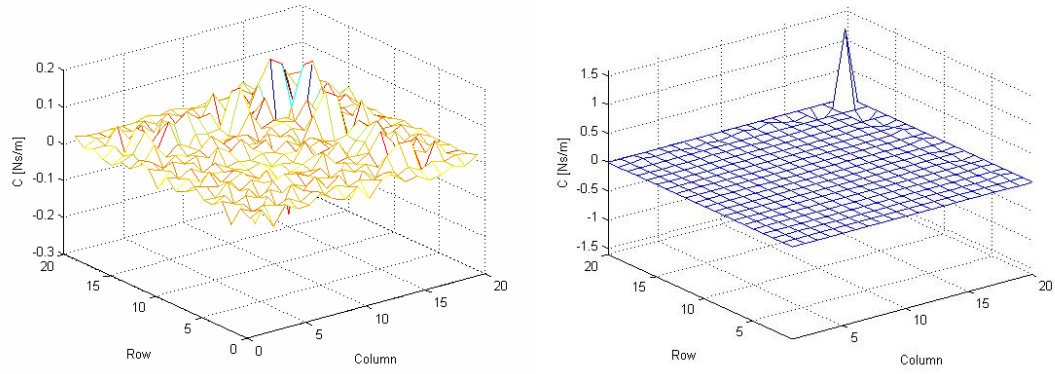
Figure 4 - Damping matrix by Adhikari's method (left) and Pilkey's method (right), 15/20 modes
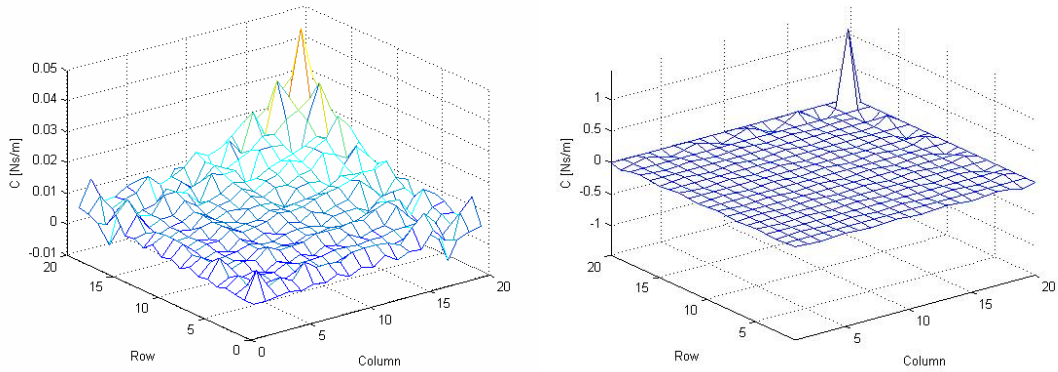

Figure 5 - Damping matrix by Adhikari's method (left) and Pilkey's method (right), 10/20 modes

These results show that Pilkey's method is less affected by this type of incompleteness than Adhikari's one. However the Frequency Response Function (FRF) obtained by using the damping matrix identified by Adhikari's method in Figure 5 reproduces well the response of the original system (Figure 6).

The FRF is obtained exciting the structure with a harmonic force

$$\mathbf{f}(t) = \mathbf{F}\, e^{i\omega t} \tag{30}$$

Substituting (30) into (2), the particular solution of the differential equation is given by

$$\mathbf{x}(t) = \mathbf{Y}\, e^{i\omega t} \tag{31}$$

The equations of motion become:

$$\left(-\omega^2\, \mathbf{M} + i\omega\, \mathbf{C} + \mathbf{K}\right)\mathbf{Y}\, e^{i\omega t} = \mathbf{F}\, e^{i\omega t} \tag{32}$$

The FRF is the mathematical expression relating the output to the input; in this case it relates displacements to exciting forces:

$$[H(\omega)] = \frac{\mathbf{x}(t)}{\mathbf{f}(t)} = \frac{\mathbf{Y}}{\mathbf{F}} = \left[-\omega^2 \mathbf{M} + i\omega \mathbf{C} + \mathbf{K} \right]^{-1} \tag{33}$$
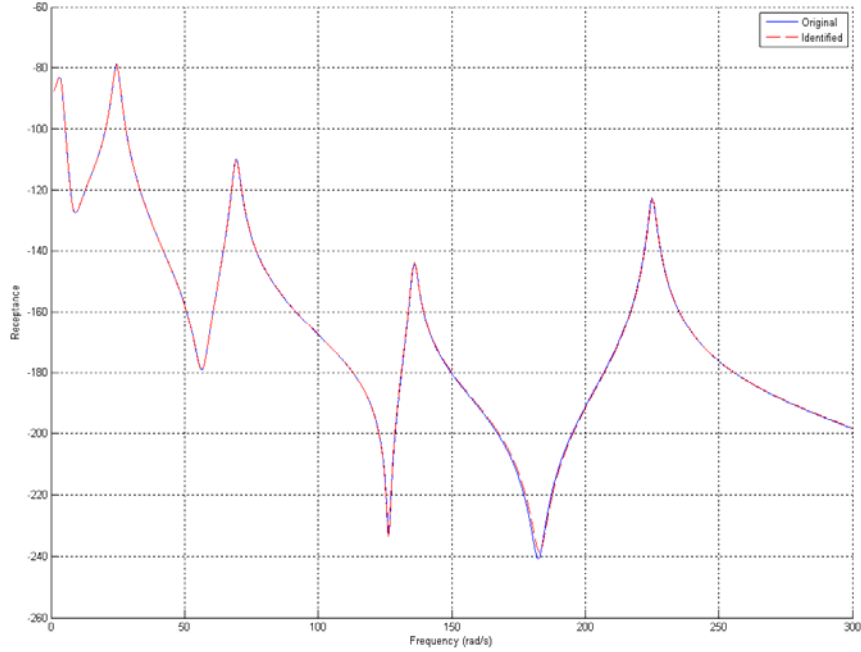

Figure 6 - FRF of the original system (blue line) and FRF of the identified (red dashed line) system using Adhikari's method, 10/20 modes

7   New method

Studying the mathematics behind Pilkey's method based on Lancaster's works [13] on the inversion of lambda-matrices and application to the theory of vibrations, a new approach was considered.

Some equations for a new model updating approach are given in reference [19]: starting from eq.(9) and rearranging eigenvalues and eigenvectors in a matrix form ($\mathbf{\Lambda}$ and $\mathbf{X}$ defined in eq.(18) and (19)) it is possible to derive some useful relations between the three system matrices:

$$\left(\mathbf{M}\mathbf{\Lambda}^2 + \mathbf{C}\mathbf{\Lambda} + \mathbf{K} \right)\mathbf{X} = 0 \tag{34}$$

In particular, three orthogonality equations can be directly derived from eq.(34) by several matrix manipulations

$$\mathbf{\Lambda}\mathbf{X}^T \mathbf{M}\,\mathbf{X}\mathbf{\Lambda} - \mathbf{X}^T \mathbf{K}\,\mathbf{X} = \mathbf{D}_1 \tag{35}$$

$$\mathbf{\Lambda}\mathbf{X}^T \mathbf{C}\,\mathbf{X}\mathbf{\Lambda} + \mathbf{\Lambda}\mathbf{X}^T \mathbf{K}\,\mathbf{X} + \mathbf{X}^T \mathbf{K}\,\mathbf{X}\mathbf{\Lambda} = \mathbf{D}_2 \tag{36}$$

$$\Lambda X^T M\, X + X^T M\, X\Lambda + X^T C\, X = D_3 \tag{37}$$

where D_1, D_2 and D_3 are diagonal matrices. Equations (35)-(37) are related to each other by

$$D_1 = D_3 \Lambda \tag{38}$$

$$D_2 = -D_3 \Lambda^2 \tag{39}$$

$$D_2 = -D_1 \Lambda \tag{40}$$

It can be shown that the modal parameters a and b [20] from the Duncan state space analysis defined as

$$a_j = x_j^T C\, x_j + 2\lambda_j x_j^T M\, x_j \tag{41}$$

$$b_j = x_j^T K\, x_j - \lambda_j^2 x_j^T M\, x_j \tag{42}$$

The a and b parameters are two constants that characterize each mode and they can be measured by traditional modal analysis experiments. They are related to the diagonal matrices as

$$D_1 = -diag\left(b_1, b_2, ..., b_{2n}\right) \tag{43}$$

$$D_2 = diag\left(b_1\lambda_1, b_2\lambda_2, ..., b_{2n}\lambda_{2n}\right) \tag{44}$$

$$D_3 = diag\left(a_1, a_2, ..., a_{2n}\right) \tag{45}$$

Equations (34)-(37) can be rearranged as

$$a_j = x_j^T C\, x_j + 2\lambda_j x_j^T M\, x_j \tag{46}$$

$$0 = x_j^T C\, x_k + \left(\lambda_j + \lambda_k\right)x_j^T M\, x_k \qquad \text{when } j \neq k \tag{47}$$

$$b_j = x_j^T K\, x_j - \lambda_j^2 x_j^T M\, x_j \tag{48}$$

$$0 = x_j^T K\, x_k - \lambda_j\lambda_k x_j^T M\, x_k \qquad \text{when } j \neq k \tag{49}$$

$$b_j\lambda_j = \lambda_j^2 x_j^T C\, x_j + 2\lambda_j x_j^T K\, x_j \tag{50}$$

$$0 = \lambda_j\lambda_k x_j^T C\, x_k + \left(\lambda_j + \lambda_k\right)x_j^T K\, x_k \qquad \text{when } j \neq k \tag{51}$$

$$\left(\lambda_j^2 M + \lambda_j C + K\right)x_j = 0 \tag{52}$$

The matrices **M**, **C** and **K** can now be derived from an updating problem, following Link's paper [20]. This approach was tested on the clamped beam test case, so the matrices can be written using the parameterization:

$$\mathbf{M} = \mathbf{M}_A + \sum_{i=1}^{n_s} \alpha_i \mathbf{M}_i \qquad (53)$$

$$\mathbf{K} = \mathbf{K}_A + \sum_{i=1}^{n_s} \beta_i \mathbf{K}_i \qquad (54)$$

$$\mathbf{C} = \mathbf{C}_A + \sum_{i=1}^{n_s} \gamma_i \mathbf{M}_{Ri} + \sum_{i=1}^{n_s} \delta_i \mathbf{M}_{Ti} + \sum_{i=1}^{n_s} \varepsilon_i \mathbf{K}_i \qquad (55)$$

where n_s is the number of substructures

$\mathbf{M}_A$, $\mathbf{K}_A$, $\mathbf{C}_A$ are the initial analytical mass, stiffness and damping matrices, obtained by FEM or simply as empty matrices.

$\mathbf{M}_i$, $\mathbf{K}_i$, $\mathbf{M}_{Ri}$ and $\mathbf{M}_{Ti}$ are respectively the mass, stiffness, rotational diagonal mass and translational diagonal mass matrices of each substructure, that are defined below.

α_i, β_i, γ_i, δ_i, ε_i are the updating parameters.

In the example of the clamped beam there are no substructures, and so each element of the ten-element model is considered as a substructure, so in this particular case, the substructure matrices can be related to the finite element model of a beam.

It's important to say that the shape of all these substructure matrices can be chosen depending on the system characteristics and engineering knowledge.

Considering the FEM mass and stiffness matrix of a beam, we have

$$\mathbf{M}_{beam} = \frac{\rho A l}{420} \begin{bmatrix} 156 & 22l & 54 & -13l \\ 22l & 4l^2 & 13l & -3l^2 \\ 54 & 13l & 156 & -22l \\ -13l & -3l^2 & -22l & 4l^2 \end{bmatrix} \qquad (56)$$

$$\mathbf{K}_{beam} = \frac{EI}{l^3} \begin{bmatrix} 12 & 6l & -12 & 6l \\ 6l & 4l^2 & -6l & 2l^2 \\ -12 & -6l & 12 & -6l \\ 6l & 2l^2 & -6l & 4l^2 \end{bmatrix} \qquad (57)$$

So, the $\mathbf{M}_i$, $\mathbf{K}_i$, matrices can be chosen as n x n matrices

$$\mathbf{M}_i = \begin{bmatrix} 0 & ... & ... & ... & 0 \\ ... & ... & ... & ... & ... \\ ... & ... & \mathbf{M}_{beam} & ... & ... \\ ... & ... & ... & ... & ... \\ 0 & ... & ... & ... & 0 \end{bmatrix} \tag{58}$$

$$\mathbf{K}_i = \begin{bmatrix} 0 & ... & ... & ... & 0 \\ ... & ... & ... & ... & ... \\ ... & ... & \mathbf{K}_{beam} & ... & ... \\ ... & ... & ... & ... & ... \\ 0 & ... & ... & ... & 0 \end{bmatrix} \tag{59}$$

All components of $\mathbf{M}_i$ and $\mathbf{K}_i$ are zero except for the involved degrees of freedom of the substructure, maintaining the proportions between the sixteen values of the beam element matrix.

The $\mathbf{M}_{Ri}$ and $\mathbf{M}_{Ti}$ matrices were chosen in a form to allow the identification of the dashpot in the translational degree of freedom of the clamped beam. In that case, looking at the structure, it's immediately recognizable that there is some damping in the translational degree of freedom so the $\mathbf{M}_{Ri}$ $\mathbf{M}_{Ti}$ matrices can be chosen using engineering knowledge as

$$\mathbf{M}_{Ri} = \begin{bmatrix} 0 & ... & ... & ... & ... & ... & ... & 0 \\ ... & ... & ... & ... & ... & ... & ... & ... \\ ... & ... & 0 & 0 & 0 & 0 & ... & ... \\ ... & ... & 0 & 1 & 0 & 0 & ... & ... \\ ... & ... & 0 & 0 & 0 & 0 & ... & ... \\ ... & ... & 0 & 0 & 0 & 1 & ... & ... \\ ... & ... & ... & ... & ... & ... & ... & ... \\ 0 & ... & ... & ... & ... & ... & ... & 0 \end{bmatrix} \tag{60}$$

$$\mathbf{M}_{Ti} = \begin{bmatrix} 0 & ... & ... & ... & ... & ... & ... & 0 \\ ... & ... & ... & ... & ... & ... & ... & ... \\ ... & ... & 1 & 0 & 0 & 0 & ... & ... \\ ... & ... & 0 & 0 & 0 & 0 & ... & ... \\ ... & ... & 0 & 0 & 1 & 0 & ... & ... \\ ... & ... & 0 & 0 & 0 & 0 & ... & ... \\ ... & ... & ... & ... & ... & ... & ... & ... \\ 0 & ... & ... & ... & ... & ... & ... & 0 \end{bmatrix} \tag{61}$$

This approach is similar to proportional damping but the fact that it's applied to each substructure and not on the whole structure allows the existence of complex mode shapes and eigenvalues.

Substituting parameterizations (58)-(61) into equations (46)-(52) we obtain a set of seven updating equations

$$
a_j - x_j^T \mathbf{C}_A x_j - 2\lambda_j x_j^T \mathbf{M}_A x_j =
$$
$$
x_j^T \left(\sum_i \gamma_i \mathbf{M}_{Ri} + \sum_i \delta_i \mathbf{M}_{Ti} + \sum_i \varepsilon_i \mathbf{K}_i \right) x_j + 2\lambda_j x_j^T \left(\sum_i \alpha_i \mathbf{M}_i \right) x_j
$$

(62)

$$
-x_j^T \mathbf{C}_A x_k - (\lambda_j + \lambda_k) x_j^T \mathbf{M}_A x_k =
$$
$$
x_j^T \left(\sum_i \gamma_i \mathbf{M}_{Ri} + \sum_i \delta_i \mathbf{M}_{Ti} + \sum_i \varepsilon_i \mathbf{K}_i \right) x_k + (\lambda_j + \lambda_k) x_j^T \left(\sum_i \alpha_i \mathbf{M}_i \right) x_k
$$

(63)

$$
b_j - x_j^T \mathbf{K}_A x_j - \lambda_j^2 x_j^T \mathbf{M}_A x_j = x_j^T \left(\sum_i \beta_i \mathbf{K}_i \right) x_j - \lambda_j^2 x_j^T \left(\sum_i \alpha_i \mathbf{M}_i \right) x_j \quad (64)
$$

$$
-x_j^T \mathbf{K}_A x_k - \lambda_j \lambda_k x_j^T \mathbf{M}_A x_k = x_j^T \left(\sum_i \beta_i \mathbf{K}_i \right) x_k - \lambda_j \lambda_k x_j^T \left(\sum_i \alpha_i \mathbf{M}_i \right) x_k \quad (65)
$$

$$
b_j \lambda_j - \lambda_j^2 x_j^T \mathbf{C}_A x_j - 2\lambda_j x_j^T \mathbf{K}_A x_j =
$$
$$
\lambda_j^2 x_j^T \left(\sum_i \gamma_i \mathbf{M}_{Ri} + \sum_i \delta_i \mathbf{M}_{Ti} + \sum_i \varepsilon_i \mathbf{K}_i \right) x_j + 2\lambda_j x_j^T \left(\sum_i \beta_i \mathbf{K}_i \right) x_j
$$

(66)

$$
-\lambda_j \lambda_k x_j^T \mathbf{C}_A x_k - (\lambda_j + \lambda_k) x_j^T \mathbf{K}_A x_k =
$$
$$
\lambda_j \lambda_k x_j^T \left(\sum_i \gamma_i \mathbf{M}_{Ri} + \sum_i \delta_i \mathbf{M}_{Ti} + \sum_i \varepsilon_i \mathbf{K}_i \right) x_k + (\lambda_j + \lambda_k) x_j^T \left(\sum_i \beta_i \mathbf{K}_i \right) x_k
$$

(67)

$$
\left(\lambda_j^2 \mathbf{M}_A + \lambda_j \mathbf{C}_A + \mathbf{K}_A \right) x_j =
$$
$$
\left(\lambda_j^2 \left(\sum_i \alpha_i \mathbf{M}_i \right) + \lambda_j \left(\sum_i \gamma_i \mathbf{M}_{Ri} + \sum_i \delta_i \mathbf{M}_{Ti} + \sum_i \varepsilon_i \mathbf{K}_i \right) + \left(\sum_i \beta_i \mathbf{K}_i \right) \right) x_j
$$

(68)

Each of eq. (62)-(68) can be written in a matrix form as

$$
\{\mathbf{d}_i\} = [\mathbf{G}_i] \begin{Bmatrix} \{\boldsymbol{\alpha}\} \\ \{\boldsymbol{\beta}\} \\ \{\boldsymbol{\gamma}\} \\ \{\boldsymbol{\delta}\} \\ \{\boldsymbol{\varepsilon}\} \end{Bmatrix} = [\mathbf{G}_i]\{\mathbf{p}\}
$$

(69)

For example, equation (64) can be written as

$$
\{\mathbf{d}_3\} = [\mathbf{G}_3]\{\mathbf{p}\}
$$

(70)

where

$$\{\mathbf{d}_3\} = \begin{Bmatrix} b_1 - x_1{}^T\mathbf{K}_A\,x_1 + \lambda_1{}^2 x_1{}^T\mathbf{M}_A\,x_1 \\ b_2 - x_2{}^T\mathbf{K}_A\,x_2 + \lambda_2{}^2 x_2{}^T\mathbf{M}_A\,x_2 \\ ... \\ b_m - x_m{}^T\mathbf{K}_A\,x_m + \lambda_m{}^2 x_m{}^T\mathbf{M}_A\,x_m \end{Bmatrix} \tag{71}$$

and

$$[\mathbf{G}_3] = \begin{bmatrix} -\lambda_1{}^2 x_1{}^T\mathbf{M}_1 x_1 & ... & -\lambda_1{}^2 x_1{}^T\mathbf{M}_n x_1 & x_1{}^T\mathbf{K}_1 x_1 & ... & x_1{}^T\mathbf{K}_n x_1 & 0 & ... & 0 \\ -\lambda_2{}^2 x_2{}^T\mathbf{M}_1 x_2 & ... & -\lambda_2{}^2 x_2{}^T\mathbf{M}_n x_2 & x_2{}^T\mathbf{K}_1 x_2 & ... & x_2{}^T\mathbf{K}_n x_2 & 0 & ... & 0 \\ ... & ... & ... & ... & ... & ... & ... & ... & ... \\ -\lambda_m{}^2 x_m{}^T\mathbf{M}_1 x_m & ... & -\lambda_m{}^2 x_m{}^T\mathbf{M}_n x_m & x_m{}^T\mathbf{K}_1 x_m & ... & x_m{}^T\mathbf{K}_n x_m & 0 & ... & 0 \end{bmatrix} \tag{72}$$

All seven equations can now be put together in a single matrix equation as

$$\begin{Bmatrix} \{\mathbf{d}_1\} \\ ... \\ ... \\ \{\mathbf{d}_i\} \\ ... \\ ... \\ \{\mathbf{d}_7\} \end{Bmatrix} = \begin{bmatrix} [\mathbf{G}_1] \\ ... \\ ... \\ [\mathbf{G}_i] \\ ... \\ ... \\ [\mathbf{G}_7] \end{bmatrix} \begin{Bmatrix} \{\boldsymbol{\alpha}\} \\ \{\boldsymbol{\beta}\} \\ \{\boldsymbol{\gamma}\} \\ \{\boldsymbol{\delta}\} \\ \{\boldsymbol{\varepsilon}\} \end{Bmatrix} \quad \text{or} \quad \{\mathbf{d}\} = [\mathbf{G}]\{\mathbf{p}\} \tag{73}$$

Finally, to obtain real system matrices, the updating parameters must be real. Writing $\{\mathbf{d}\}$ and $[\mathbf{G}]$ as complex quantities and $\{\mathbf{p}\}$ as a real quantity we obtain

$$\{\mathbf{d}_{real} + i\mathbf{d}_{imag}\} = [\mathbf{G}_{real} + i\mathbf{G}_{imag}]\{\mathbf{p}\} \tag{74}$$

and it's possible to separate the real and the imaginary parts obtaining the final matricial equation

$$\begin{Bmatrix} \mathbf{d}_{real} \\ \mathbf{d}_{imag} \end{Bmatrix} = \begin{bmatrix} \mathbf{G}_{real} \\ \mathbf{G}_{imag} \end{bmatrix}\{\mathbf{p}\} \implies \{\mathbf{q}\} = [\mathbf{S}]\{\mathbf{p}\} \tag{75}$$

If m modes are correctly measured, we are able to write a total of $8m^2$ equations.
The updating parameters can now be calculated using the linear least squares optimization technique by the pseudo-inverse

$$\{\mathbf{p}\} = (\mathbf{S}^T\mathbf{S})^{-1}\mathbf{S}^T\{\mathbf{q}\} \tag{76}$$

and is used to reconstruct the three identified matrices.

This new method was numerically tested on the test problem with modal incompleteness and it gave good results using only 4 out of 20 modes (Figure 7). These initial results are encouraging.
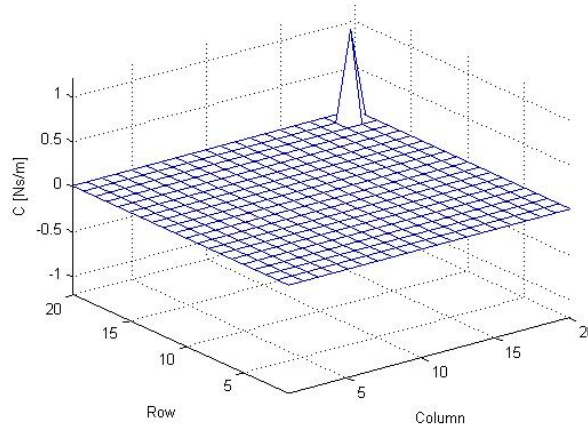

Figure 7 - Damping matrix identified by new approach, 4 out of 20 modes

7.1   Comparison between the three methods

Results obtained by the three methods were compared using two measures of error for the number of modes used in identification.

The first measure is called "amplitude error" and it defines how much the identified matrix differs from the original one in terms of amplitude.

This is simply obtained by dividing the Frobenius norm of the difference between the original matrix and the identified one by the Frobenius norm of the original matrix, and multiplying by 100.

$$e_{amp}(\%) = \frac{\left\| C_{original} - C_{identified} \right\|_F}{\left\| C_{original} \right\|_F} \cdot 100 \tag{77}$$

Figure 8 shows that Adhikari's method has strange behaviour with bigger error when using almost all modes and a sort of stabilization of errors under a certain number (fifteen). Results obtained by Pilkey's method, in contrast, increase their quality with an increasing number of modes, as expected.

The new method seems to work perfectly, but it must be said that all the information about the structure under consideration were known and it was easy to choose the right substructure matrices for this example.

The second error is called "localization error" and it represents the distance from the highest values of the identified matrices to the correct position of the dashpot (in this case: 19th row and 19th column of the damping matrix).
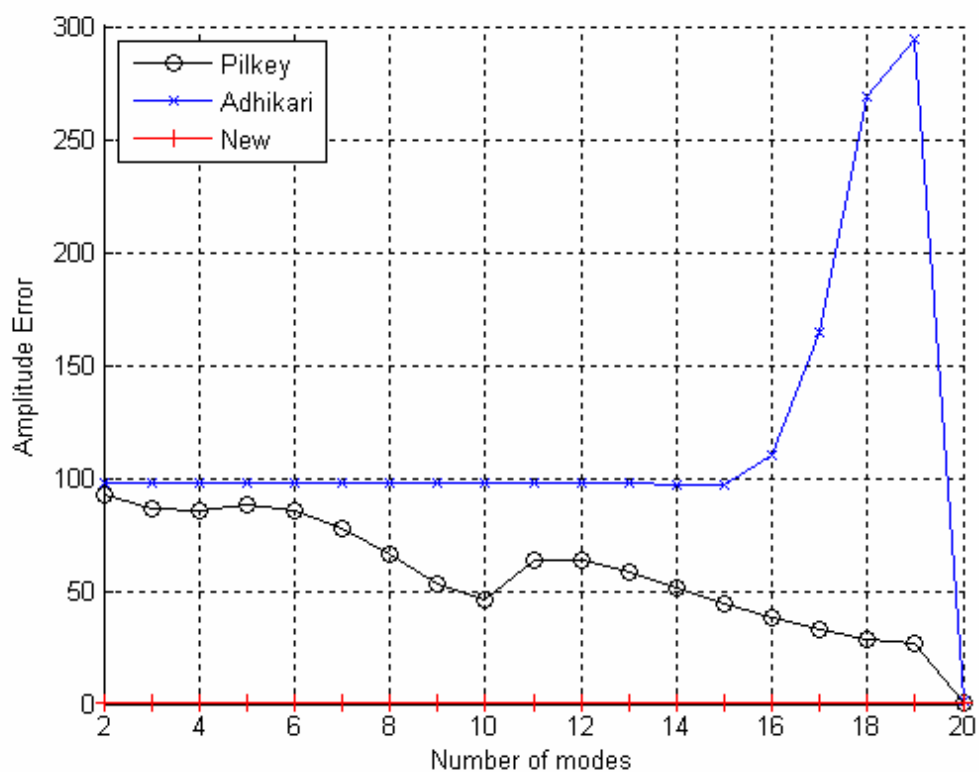
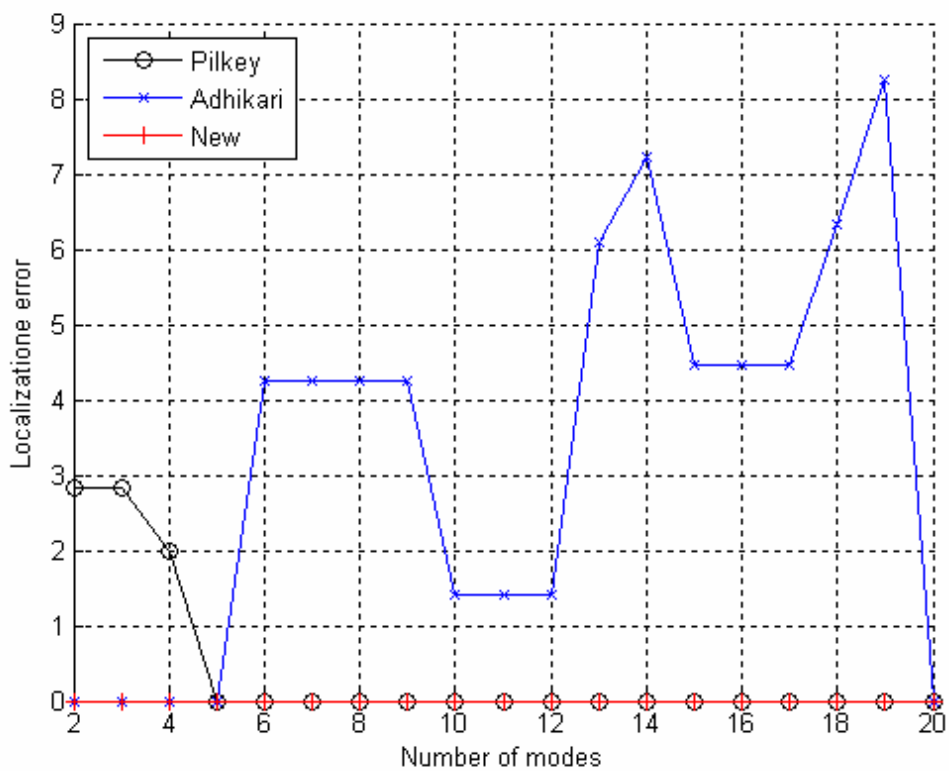**Figure 8** - Amplitude error comparison between the three methods

Figure 9 - Localization error comparison between the three methods

If r_o and c_o are respectively the row and the column where the dashpot is located in the original matrix and r_i and c_i are respectively the row and the column of the identified matrix where the highest value is obtained, the "localization error" is defined as a distance by

$$e_{loc} = \sqrt{\left|r_o - r_i\right|^2 + \left|c_o - c_i\right|^2} \tag{78}$$

In Figure 9 the same strange behaviour is shown by Adhikari's method which seems to work better using less than 5 modes instead of 19. The other two methods show better results for increasing the number of modes.

It could be interesting to investigate not just how many modes could be used to identify damping but also which ones are the best to be used in the process, because it is shown that adding more modes sometimes gives worst results in the identification.

8 Conclusions

In the present report a survey of some existing damping identification methods has been presented and a new method based on orthogonality equations has been considered. The three methods were evaluated for a test problem to show how much they are affected by one of the main problems in identification: the modal incompleteness of data.

Results shows that Adhikari's method has strange behaviour with bigger error when using almost all modes and seems strongly affected by this type of incompleteness. Pilkey's method increases its quality with an increasing number of modes, as expected.

Results obtained by the new method were encouraging and look better than the two existing methods. However, the example is simple and further investigations are needed.

Future work includes a deeper investigation on the new approach and in particular:

- Test the new approach with more complex structures in order to validate it and to present standard substructure matrices to be used in real tests.
- Test the new approach with real structures.
- Comparing the three different models with real structures.
- Investigate the spatial incompleteness problem (model reduction or modal expansion) in order to optimize the measurement from real experiments (this includes criterions to select the best place to put accelerometers).
- How to separate the different types of damping and how to model each of them.

More complex structures can be designed using more than one beam connected with joints that creates different types of damping.

To obtain hi-fidelity models from the data obtained by Ground Vibration Test, an important issue is to separate the different sources of damping in the identification process in order to model them separately and more accurately.

In the recent Ecerta meeting in Turin this idea was discussed and a collaboration with Politecnico di Torino could start on this topic with a modal analysis experiment on a beam with different sources of damping; the final target will be to define a procedure which makes possible the extraction of separated coefficients for viscous damping, Coulomb

friction damping and any other source present in a wing using Ground Resonance Tests data.

The separation of the sources of damping is a very important task because is still not clear which type of damping is the most important and it could be very useful to evaluate how much each type of damping contributes to the global value and which one can be neglected. Another idea, still not developed, is to introduce random matrix theory in damping identification.

9 References

[1] ADHIKARI S., "Damping models for structural vibration", *PhD thesis*, University of Cambridge, p.1, 2000.

[2] GAUL L., "The influence of damping on waves and vibrations", *Mechanical systems and signal processing*, **13**(1), pp. 1–30, 1999.

[3] WOODHOUSE J., "Linear damping models for structural vibration", *Journal of sound and vibration*, **215**(3), pp. 547-569, 1998.

[4] BISPLINGHOFF R.L., ASHLEY H. and HALFMAN R.L., "Aeroelasticity", Dover Publications, New York, 1996.

[5] NJUGUNA J., " Flutter prediction, suppression and control in aircraft composite wings as a design prerequisite: A survey", *Structural Control and Health Monitoring*, **14**, pp. 715-758, 2006.

[6] RAYLEIGH L., "Theory of sound", Dover Publications, New York, reissued, 1945.

[7] MAIA N.M.M., SILVA J.M.M., HE J., LIEVEN N.A.J., LIN R.M., SKINGLE G.W., TO W.M., URGUEIRA A.P.V., "Theoretical and experimental modal analysis", Research Studies Press, 1997.

[8] ADHIKARI S. and WOODHOUSE J., "Identification of damping: part 1, viscous damping", *Journal of Sound and Vibration*, **243**(1), pp. 43-61, 2001.

[9] ADHIKARI S., "Damping models for structural vibration", *PhD thesis*, University of Cambridge, 2000.

[10] LEES A.W., "Use of perturbation analysis for complex modes", *Proceedings of the 17th International Modal Analysis Conference*, Vol. 3727, p. 779, 1999.

[11] PILKEY F.D., PARK G. and INMAN D.J., "Damping matrix identification and experimental verification", *Proceedings of the SPIE's 6th Annual International Symposium on Smart Structures and Materials*, Newport Beach, California Vol. 3672, pp. 350-357, 1999.

[12] LANCASTER P., "Expression of damping matrices in linear vibrations problems", *Journal of the aerospace science*, Vol.28, p. 256, 1961.

[13] LANCASTER P. and PRELLS U., "Inverse problems for damped vibrating systems", *Journal of Sound and Vibration*, **283**, pp. 891-914, 2005.

[14] FRISWELL M.I. and MOTTERSHEAD J.E., "Finite Element Model Updating in Structural Dynamics", Kluwer Academic Publishers, p. 65, 1995.

[15] GUYAN R.J., "Reduction of stiffness and mass matrices", *Journal of American Institute of Aeronautics and Astronautics*, **3**, p. 280, 1965.

[16] PAZ M., "Dynamic condensation", *Journal of American Institute of Aeronautics and Astronautics*, Vol.22, **5**, pp. 724-727, 1984.

[17] O'CALLAHAN J.C., "A procedure for an improved reduced system (IRS) model", *Proceedings of the 7th International Modal Analysis Conference*, Las Vegas, 1989.

[18] O'CALLAHAN J.C. P. AVITABILE, and R. RIEMER, " System equivalent reduction expansion process (SEREP)", *Proceedings of the 7th International Modal Analysis Conference*, Las Vegas, pp. 29-37, 1989.

[19] DATTA B.N., ELHAY S. and RAM Y.M., "Orthogonality and partial pole assignment for the symmetric definite quadratic pencil", *Linear algebra and its applications*, **257**, pp. 29-48, 1997.

[20] Link M., "Using complex modes for model updating of structures with non proportional damping", *Proceedings of the International Conference on Noise and Vibration Engineering (ISMA2006)*, University of Leuven, Belgium, September 2006.

[21] Ho S., Nassef H., Pornsinsirirak N., Tai Y.C., Ho C.M., "Unsteady aerodynamics and flow control for flapping wing flyers", *Progress in Aerospace Sciences*, **39**, pp. 635-681, 2003.